Kinetically guided radical-based synthesis of $C(sp^3)$–$C(sp^3)$ linkages on DNA

Jie Wang[a,1], Helena Lundberg[a,1], Shota Asai[a], Pedro Martín-Acosta[a], Jason S. Chen[a], Stephen Brown[b], William Farrell[c], Russell G. Dushin[b], Christopher J. O'Donnell[b], Anokha S. Ratnayake[b], Paul Richardson[c], Zhiqing Liu[d], Tian Qin[a], Donna G. Blackmond[a,2], and Phil S. Baran[a,2]

[a]Department of Chemistry, The Scripps Research Institute, La Jolla, CA 92037; [b]Natural Products Laboratory, Worldwide Medicinal Chemistry, Pfizer Worldwide Research and Development, Groton, CT 06340; [c]Department of Chemistry, La Jolla Laboratories, Pfizer Inc., San Diego, CA 92121; and [d]Tianjin Key Laboratory of Pharmaceutical Green Synthesis Technology, Asymchem Laboratories (Tianjin) Co., Ltd., Tianjin 300457, P. R. China

Contributed by Phil S. Baran, May 31, 2018 (sent for review April 24, 2018; reviewed by Will Gutekunst and Jason Hein)

DNA-encoded libraries (DEL)-based discovery platforms have recently been widely adopted in the pharmaceutical industry, mainly due to their powerful diversity and incredible number of molecules. In the two decades since their disclosure, great strides have been made to expand the toolbox of reaction modes that are compatible with the idiosyncratic aqueous, dilute, and DNA-sensitive parameters of this system. However, construction of highly important $C(sp^3)$–$C(sp^3)$ linkages on DNA through cross-coupling remains unexplored. In this article, we describe a systematic approach to translating standard organic reactions to a DEL setting through the tactical combination of kinetic analysis and empirical screening with information captured from data mining. To exemplify this model, implementation of the Giese addition to forge high value C–C bonds on DNA was studied, which represents a radical-based synthesis in DEL.

DNA-encoded libraries | combinatorial chemistry | radical reactions | organic synthesis | kinetic analysis

Brenner and Lerner's (1) now landmark 1992 PNAS disclosure provided the intellectual blueprint and proof of concept (2–4) for a new type of combinatorial chemistry that could be encoded by DNA, setting the stage for the synthesis of DNA-encoded libraries (DEL). This prescient report foresaw the benefits of combining the powerful diversity enabled by chemical synthesis with the errorless labeling and amplification of genetic techniques (5–9). In this way, libraries of incredible size (up to $>10^9$ members) could be procured and screened at once (rather than one by one in traditional combinatorial chemistry) with the ultimate vision of democratizing the practice of medicinal chemistry (10–15). The vision and principles outlined therein are only recently being realized with advances in analysis and chemoselective synthesis, setting the stage for the widespread adoption of DEL-based discovery platforms in the pharmaceutical arena (16–20). DNA-compatible synthesis provides exciting challenges (21–23), particularly as most traditional techniques are not amenable to the idiosyncratic requirements of such systems (24, 25). As outlined in Fig. 1*A*, the rules associated with routine organic synthesis must be rewritten when transitioning to a DEL. For example, the limitations of DNA solubility require several orders of magnitude difference in both the concentrations of reaction components (*ca.* 0.1 M vs. 0.001 M) and water content (parts per million vs. 20+% vol) of the solvents employed. For the purposes of a standard medicinal chemistry program, as little as 5% yield might be acceptable to obtain a biological readout, whereas each DEL-based step must proceed in at least 40% yield, as purification in between steps is not an option due to mixed millions of compounds employed in the latter regime. In a similar vein to radiochemistry, the concept of atom economy in DEL is not applicable, as the library, usually prepared from less than 100 μmol of DNA (26), can be used multiple times solely for discovery purposes, and thus the only important consideration is to maximize the yield. The final, and perhaps most challenging constraint, is the reaction conditions do not damage the functional group-rich DNA-based barcode because such an event would undermine the value of the entire library. As such, conventional wisdom teaches that the pH range must reside between 4 and 14, the temperature should not exceed 90 °C (27), and strong oxidants and radical chemistry (24, 28) should be avoided. Thus, DEL-based synthesis represents a perfect storm of requirements that has, to date, prevented the vast majority of organic transformations from being enlisted.

In an effort to expand the diversity of available reactions for use in DEL, methods were sought to forge C–C bonds with enhanced 3D shape through a cross-coupling strategy (29) (Fig. 1*B*). Historically, amide bond formation (the very first DEL-based reaction) (2–4) and reductive amination have been the workhorse reactions for C–N bond formation in DEL (10, 30–32). In contrast, C–C bond formation is relatively less employed, with the most popular reactivity modes disclosed involving two-electron processes such as arene–arene Suzuki coupling (33), olefin metathesis (34), aldol condensation (35), and cycloaddition (36). Conjugate addition, one of the most oft-employed transformations in organic synthesis (37, 38), is notably absent from this list (39, 40). In principle, such a reaction would provide an orthogonal set of diverse $C(sp^3)$–$C(sp^3)$ linkages from simple

Significance

Combinatorial synthesis via DNA encoded library (DEL) has evolved as a technology of great importance in drug discovery. However, the idiosyncratic aqueous, dilute, DNA-sensitive parameters and infinitesimal scale of this system present new challenges for traditional organic reactions. A detailed protocol aiding the transition from organic reactions to reactions with DNA-bound molecules was developed using a tactical combination of kinetic analysis and reaction screening. As an example, the venerable Giese addition was applied to forge high-value C–C bonds, including all-carbon quaternary centers, on DNA, representing the first radical-based synthesis in DEL that expands the traditional toolbox beyond pericyclic, carbonyl-based, and two-electron cross-couplings.

Author contributions: J.W., H.L., R.G.D., T.Q., D.G.B., and P.S.B. designed research; J.W., H.L., S.A., P.M.-A., and S.B. performed research; Z.L. contributed new reagents; J.W., H.L., S.A., P.M.-A., J.S.C., S.B., W.F., C.J.O., A.S.R., and P.R. analyzed data; and J.W., H.L., T.Q., D.G.B., and P.S.B. wrote the paper.

Reviewers: W.G., Georgia Tech; and J.H., University of British Columbia.

Conflict of interest statement: S.B., W.F., R.G.D., C.J.O., A.S.R., and P.R. are full-time employees of Pfizer Inc. D.G.B. and P.S.B. have received research funding from Pfizer Inc.

[1]J.W. and H.L. contributed equally to this work.

[2]To whom correspondence may be addressed. Email: blackmon@scripps.edu or pbaran@scripps.edu.

This article contains supporting information online at www.pnas.org/lookup/suppl/doi:10.1073/pnas.1806900115/-/DCSupplemental.

Published online June 26, 2018.

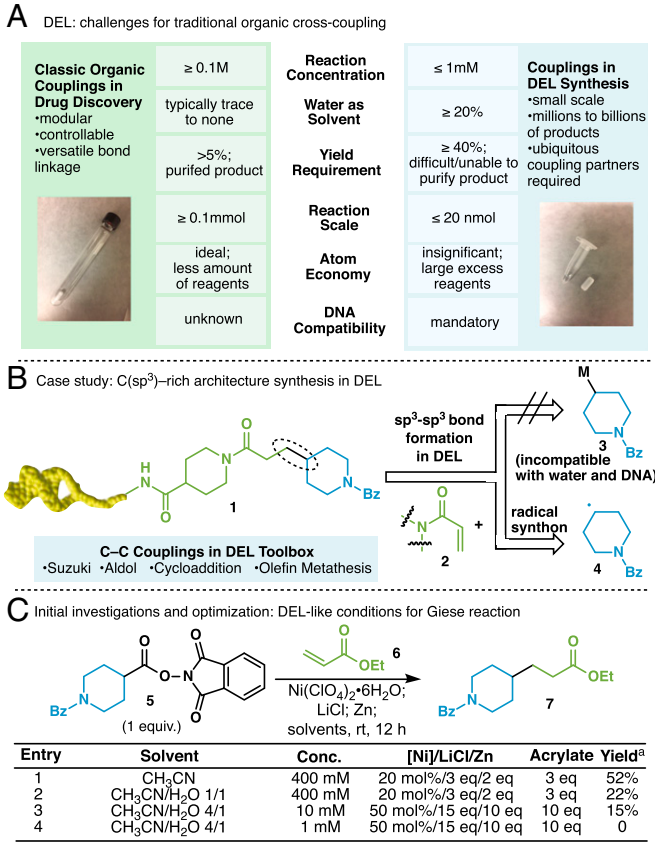

Entry	Solvent	Conc.	[Ni]/LiCl/Zn	Acrylate	Yield[a]
1	CH_3CN	400 mM	20 mol%/3 eq/2 eq	3 eq	52%
2	CH_3CN/H_2O 1/1	400 mM	20 mol%/3 eq/2 eq	3 eq	22%
3	CH_3CN/H_2O 4/1	10 mM	50 mol%/15 eq/10 eq	10 eq	15%
4	CH_3CN/H_2O 4/1	1 mM	50 mol%/15 eq/10 eq	10 eq	0

[a] Yields were determined by LC/UV with 1,3,5-trimethoxybenzene as internal standard.

Fig. 1. DEL presents new challenges for traditional organic transformation. (*A*) DEL: challenges for traditional organic cross-coupling. (*B*) Case study: C (sp^3)-rich architecture synthesis in DEL. (*C*) Initial investigations and optimization: DEL-like conditions for Giese reaction.

building blocks. In its traditional manifestation, this two-electron process requires a metallated organic fragment and is thus completely incompatible with DEL. [A few exceptions for cross-coupling reactions using anionic pre-formed organometallic reagents have been reported, although at considerably higher concentrations than those required for DEL synthesis (for example, see refs. 41 and 42).] In contrast, the conjugate addition of one-electron species in a Giese-type union under aqueous conditions is known using genotoxic alkyl halide reagents as coupling partners (43–46). Recent studies have demonstrated that the same disconnection can be accomplished through a tactically different one-electron strategy using ubiquitous carboxylic acids (47–49) as latent nucleophiles with Michael acceptors (50–52). This potentially powerful disconnection was explored, despite the known sensitivity of DNA to radicals (24, 28), in the hopes that a judicious choice of reaction conditions could solve this issue. Unfortunately, and not surprisingly, initial studies to adapt this transformation to DEL-like conditions failed, with complete inhibition by the highly dilute aqueous conditions (Fig. 1*C*). Rather than discarding the approach, a mechanistic analysis was pursued to understand the driving forces and underlying causes of this setback. In this report, a straightforward kinetically guided paradigm is presented for the rapid interrogation and translation of organic reactions to DEL compatibility leading to a radical-based reaction for DNA-based synthesis programs.

The demonstrated incompatibility of the decarboxylative Giese reaction to mock-DEL conditions represented an opportunity to develop a mechanistically guided approach for rendering organic reactions amenable to the challenges outlined above (Fig. 1*A*). The goal was to develop a stepwise systematic protocol that could, in principle, be generalized to a variety of organic reactions as illustrated in Fig. 2*A*. This process proceeds through simple sequential steps and can result in both the successful transition to DEL-like conditions and an enhanced understanding of the canonical organic reaction. Step 1 involves prioritizing reactions for study that do not have extreme air or moisture sensitivity. In Step 2, the protocols of Reaction Progress Kinetic Analysis (RPKA) (53–55) are applied under the parent organic conditions to determine concentration driving forces. The data obtained in this analysis then help guide the selection of initial conditions to identify a suitable DEL-compatible protocol for reactants and reagents, particularly as they relate to the extremely dilute conditions. In Step 3, an empirical evaluation of solvents, additives, and temperatures can take place wherein the progress of all reactions is monitored over time. The temporal data obtained are extremely valuable when graphically visualized, to help uncover hidden patterns and trends that may lead to improved conversion to product as well as provide mechanistic insight. Guided by this data-mining procedure, starting conditions are chosen in Step 4 for an iterative evaluation of compatibility with DNA. Success in Step 4 leads to an evaluation of the scope in Step 5 as a prelude to transitioning to a DEL platform in Step 6.

This process as applied to the Giese reaction is outlined in Fig. 2 *B*–*D*. RPKA analysis shows that the reaction rate depends on neither the redox active ester (RAE) nor acrylate substrate concentrations under organic conditions. In addition, increasing the concentration of the Ni did not increase the rate. The sole variables affecting rate were the concentration of LiCl and the quantity of Zn powder. These findings suggest that the reaction may involve a step that depends on the available surface area of Zn, and the Li salt may act as an electrolyte to facilitate electron transfer through the organic medium. The unusual zero-order behavior in substrate concentrations (under conditions where it has been established that mass transfer limitations have been minimized; see *SI Appendix*) suggests a radical process that, once initiated, propagates the reaction without depending on the concentration of reaction components, or a heterogeneous reaction that proceeds on a surface fully occupied by substrates. Hence, the kinetic analysis suggests that the Giese reaction is amenable to DEL conditions. In general, a reaction that exhibits zero or low positive-order kinetics in reactants has the potential for being scaled to dilute concentrations without adversely affecting the rate.

Following these experiments, we began to screen reactions to evaluate the role of different components under the dilute aqueous conditions required for preparing DNA encoded libraries using a high LiCl concentration and a large surface area of Zn, the reagents that exhibited positive driving forces under organic conditions. We screened a range of variables, including reactant and catalyst concentrations, different metal powders, buffers, surfactants, and solvent ratios (*SI Appendix*). We observed that the RAE substrate is rapidly consumed, even in reactions that gave low yield to the desired reaction product. In addition, some reactions proceeded much slower than others in terms of both RAE consumption and desired product yield. These observations indicate that a simple measurement of final yield at a given reaction time does not capture all of the critical information about reaction pathways in this system. To extract information to optimize desired product formation, we combined the voluminous data from all time course screening experiments into a single selectivity chart that helps to collate and standardize the data by correlating RAE consumption with desired product formation at each given point in time under each set of conditions, as shown in Fig. 2*C*. Thus, the dashed diagonal line represents a reaction where all of the limiting substrate is converted to desired product, i.e., an "ideal" reaction. Plotting the data in this way allowed us to remove reaction time as a variable and rapidly elucidate the relationships between a range

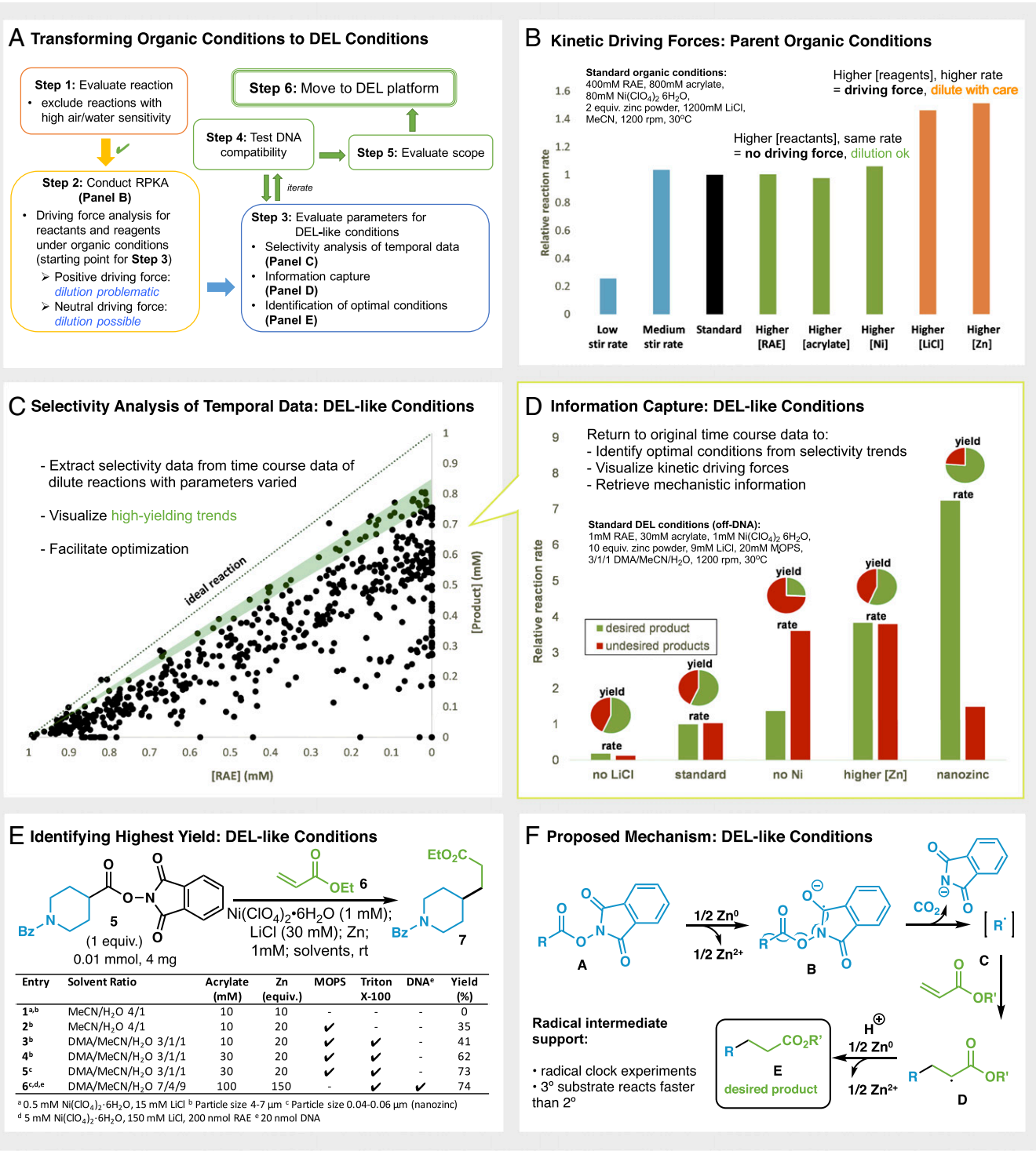

Entry	Solvent Ratio	Acrylate (mM)	Zn (equiv.)	MOPS	Triton X-100	DNA[e]	Yield (%)
1[a,b]	MeCN/H_2O 4/1	10	10	-	-	-	0
2[b]	MeCN/H_2O 4/1	10	20	✔	-	-	35
3[b]	DMA/MeCN/H_2O 3/1/1	10	20	✔	✔	-	41
4[b]	DMA/MeCN/H_2O 3/1/1	30	20	✔	✔	-	62
5[c]	DMA/MeCN/H_2O 3/1/1	30	20	✔	✔	-	73
6[c,d,e]	DMA/MeCN/H_2O 7/4/9	100	150	-	✔	✔	74

[a] 0.5 mM $Ni(ClO_4)_2 \cdot 6H_2O$, 15 mM LiCl [b] Particle size 4-7 μm [c] Particle size 0.04-0.06 μm (nanozinc)
[d] 5 mM $Ni(ClO_4)_2 \cdot 6H_2O$, 150 mM LiCl, 200 nmol RAE [e] 20 nmol DNA

Fig. 2. Translating standard organic reactions to a DEL setting through the tactical combination of RPKA and empirical screening. (*A*) Transforming organic conditions to DEL-like conditions. (*B*) Kinetic driving force: parent organic conditions. (*C*) Selectivity analysis of temporal data: DEL-like conditions. (*D*) Information capture: DEL-like conditions. (*E*) Identifying highest yield: DEL-like conditions. (*F*) Proposed mechanism: DEL-like conditions.

of parameters to optimize conditions for highest yield of desired product. Manipulating the data in this way allows us to visualize clusters of optimal reaction conditions. For example, the high-yielding trends shown in the green swath pinpointed higher Zn concentrations, and, in particular, the use of nanozinc to increase yield. Following this analysis, we returned to the original time course data for selected points in Fig. 2*C* to decode the trends in the selectivity analysis plot and identify the factors of importance for achieving high yields of the desired product, as well as to extract rates and mechanistic information using RPKA methodology. For example, Fig. 2*D* highlights results for rate and yield of both desired and undesired products obtained from selected reaction conditions in Fig. 2*C*. The bar diagrams indicate that the absence of LiCl reduces the rate of reaction whereas the

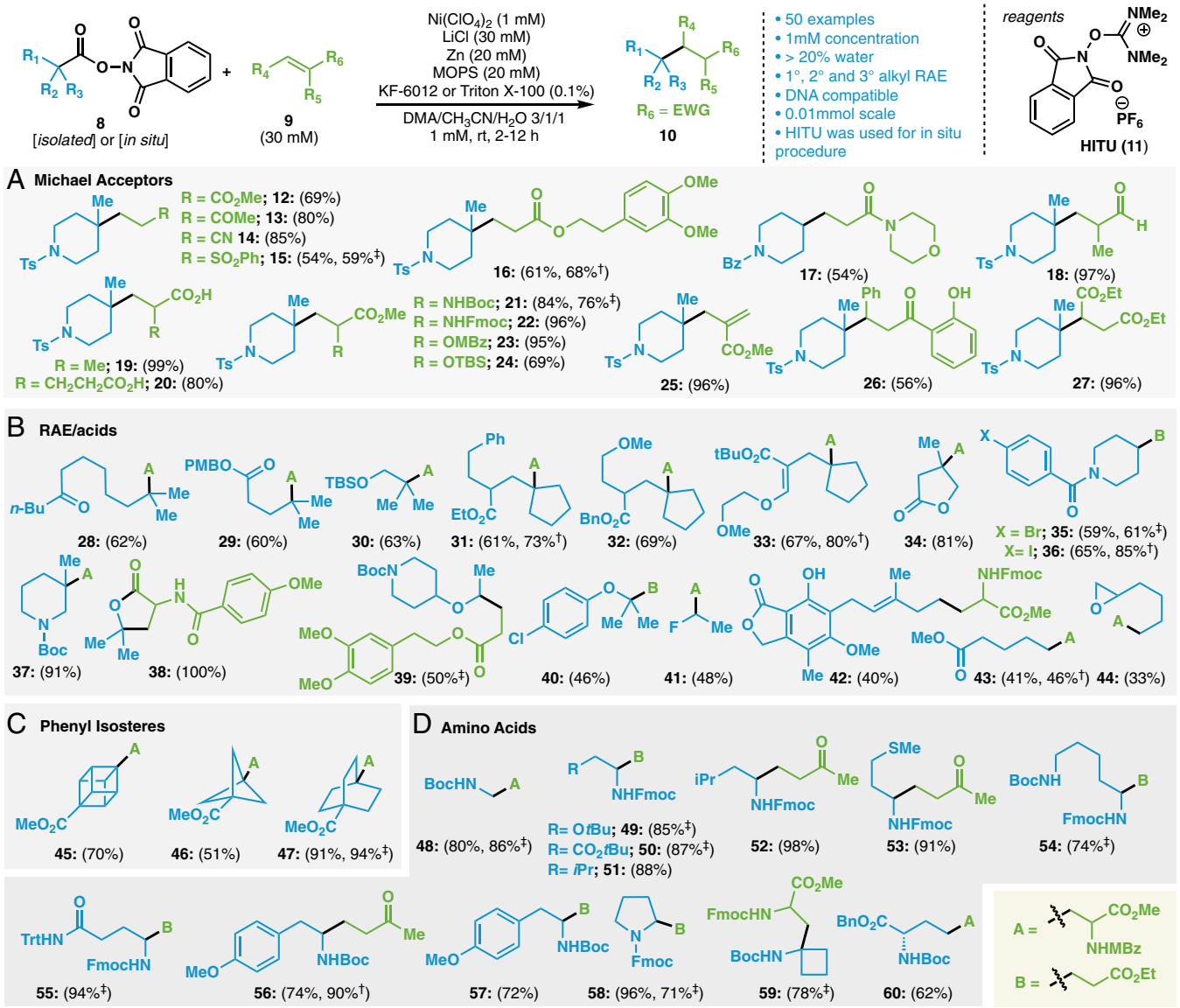

Fig. 3. Substrate scope utilizing DEL-like conditions. (*A*) Michael acceptors. (*B*) RAE/acids. (*C*) Phenyl isosteres. (*D*) Amino acids. See *SI Appendix* for experimental details. Dagger (†) denotes that zinc nanopowder was used. Double dagger (‡) denotes that RAE was generated in situ.

selectivity remains unaltered, consistent with this component acting as an electrolyte in the system. Furthermore, the rate of product formation remains the same in both the absence and presence of nickel, whereas selectivity suffers significantly in the former case. In analogy with the parent organic conditions, the surface area of Zn is a driving force under DEL conditions, as indicated by the higher rates using either a higher amount of Zn with the same particle size or the same amount of higher surface area Zn nanoparticles. Gratifyingly, the use of the latter form of Zn increased the rate of product formation without affecting byproduct formation, resulting in the highest yields of desired product observed in the screening. The translatability of the kinetic trends for the parent organic conditions to DEL conditions indicates that the same mechanism is operating and further suggests that conclusions drawn from reactions using DEL conditions off-DNA will likely be applicable to their on-DNA counterparts.

From the data in Fig. 2*C*, trends for achieving high yields can be highlighted. Key findings (see *SI Appendix* for complete discussion) are summarized in Fig. 2*E* and include (*i*) more Zn and the use of MOPS buffer (Entry 2 vs. Entry 1), (*ii*) addition of surfactant (Entry 3 vs. Entry 2), (*iii*) increased acrylate concentration (Entry 4 vs. Entry 3), and (*iv*) use of zinc with a greater surface area (Entry 5 vs. Entry 4). Finally, the conditions derived from Entry 5 could be performed in the presence of DNA with no effect on yield and minimal degradation of the DNA (Entry 6).

The combined kinetic data under DEL-like conditions and literature precedence (for alkyl radical generated from *N*-hydroxyphthalimide esters via single electron-transfer, see, for example, refs. 56 and 57) allow the proposal of the productive reaction mechanism (Fig. 2*F*). The RAE is reduced via electron transfer from Zn, resulting in the formation of a radical anion that fragments into a carbon-centered radical that reacts with the acrylate in a Giese-type 1,4-addition. Thus, the protocol outlined in Fig. 2 provides a recipe for identifying, applying, and understanding reactions that are potentially useful for a DEL synthesis. This sets the stage for the two final steps, namely, evaluating the scope of DEL-like conditions and actual application to synthesis on DNA.

With a viable set of DEL-like conditions in hand, the Giese coupling was evaluated with the goal of broadening the scope to

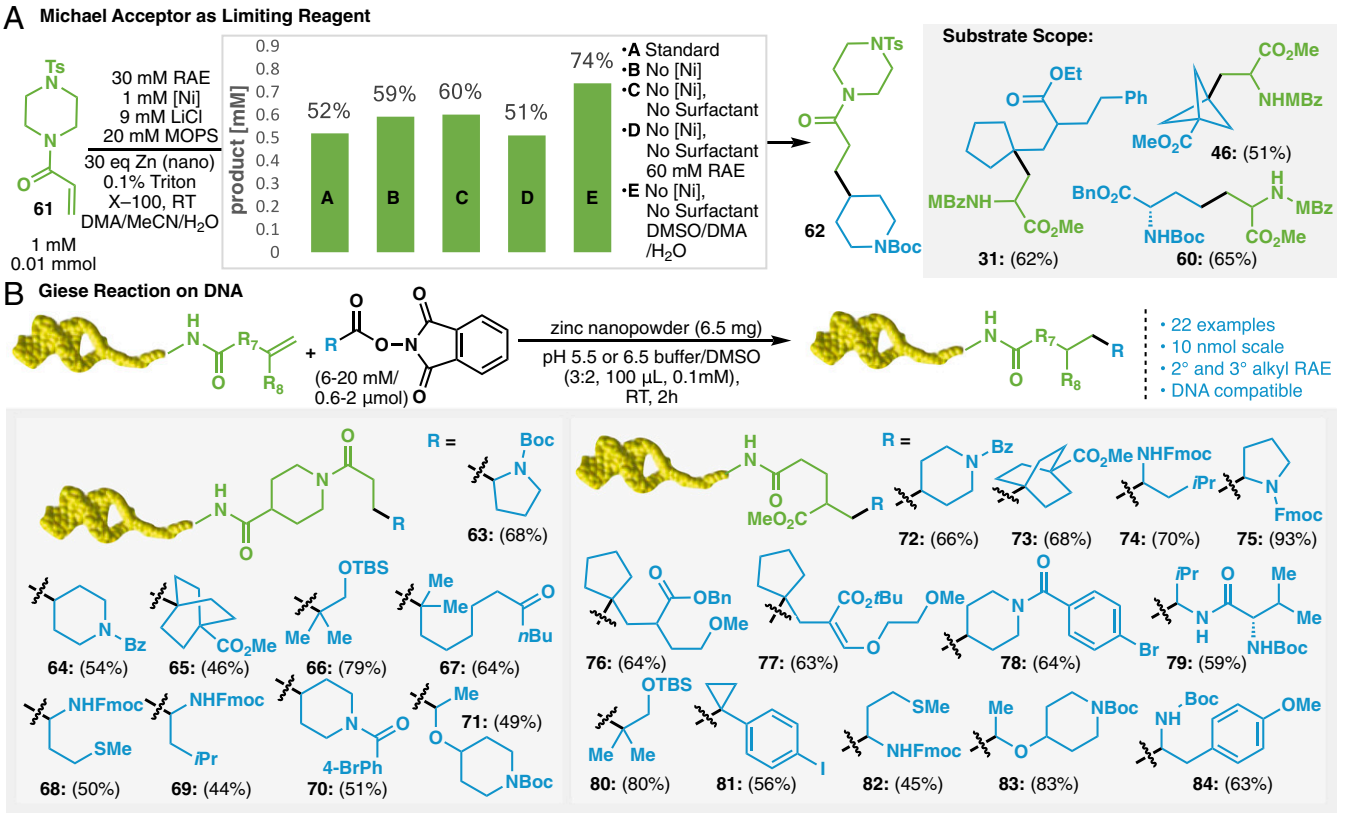

Fig. 4. From DEL-like conditions to Giese reaction on DNA-bound molecule. (*A*) Michael acceptor as limiting reagent. (*B*) Giese reaction on DNA.

include medicinally attractive C(sp^3) architectures and versatile functionality for use in subsequent diversification. For simplicity, the majority of reactions were conducted with standard zinc powder, although nanozinc was uniformly demonstrated to give higher yields. The optimized protocol was applied to over 50 substrates (Fig. 3 *A*–*D*), only 7 of which have been reported before under standard organic conditions. The scope of Michael acceptors (Fig. 3*A*) was probed first; to this end, acrylates (**12**, **16**), acrylamides (**17**), vinyl ketones (**13**), acrylonitriles (**14**), and vinyl sulfones (**15**) were all found to be competent radical acceptors. Both α-substituted (**18**–**24**) and β-substituted (**26**, **27**) acceptors could be employed in this protocol, providing the Giese products in excellent yields. Reactive functional groups such as aldehydes (**18**) and acids (**19**, **20**) were tolerated in this coupling, allowing them to serve as handles for a variety of DEL-compatible downstream functionalizations (e.g., reductive amination or amide-bond formation, respectively). Moreover, acrylates with a CH_2SO_2Tol in the α-position underwent elimination following radical addition (58), leading to another Michael acceptor moiety (**25**) and making the process amenable for iterative multicycle C–C bond forming Giese in a DEL context.

As DEL logic features the tandem preparation of multiple compounds in a single flask without recourse to conventional purification techniques, a broad scope with respect to RAE and compatibility with different functionality is therefore of paramount importance. Thus, a diverse selection of carboxylic acids curated from the Pfizer inventory were identified and examined under the DEL-like conditions. Toward that end, a broad range of C(sp^3)–C(sp^3) linked products from 33 unique alkyl carboxylic acids or their redox-active ester derivatives were prepared. Primary (**42**–**44**, **48**, **60**), secondary (**35**, **36**, **39**, **41**, **49**–**58**), and tertiary (**28**–**34**, **37**, **38**, **40**, **45**–**47**, **59**) carboxylic acids were all amenable to coupling. Dehydroalanine as an olefin partner delivered a variety of exotic unnatural amino acids (**28**–**34**, **37**, **38**, **41**, **43**–**48**, **60**). Sensitive functional groups that are potentially intolerant of reductive conditions or nonphysiological pH, such as alkyl enol ethers (**33**), halides (chloride in **40**, bromide in **35**, iodide in **36**), Fmoc protecting groups (**42**, **49**–**55**, **58**), thioethers (**53**), olefins (**42**), benzyl esters (**32**), and epoxides (**44**), were found to remain intact.

Cubanes (59), propellanes (60, 61), and [2,2,2]-bicyclooctanes (62) of various substitution patterns have been shown to be important phenyl bioisosteres in medicinal chemistry; however, their broad incorporation into DEL platforms is hindered by a lack of C–C bond forming methods. Fig. 3*C* demonstrates that decarboxylative coupling at the uniquely bridged carbon of these medicinally popular scaffolds provided a straightforward method to incorporate the aforementioned moieties (**45**–**47**). Both β- (**34**, **37**) and α- (free OH, **38**; O, **39**, **40**; F, **41**; N, **48**–**59**) heteroatoms substituted acids were converted to coupling products smoothly.

Amino acids play an important role in DEL-based drug discovery; the acid moiety was often employed as a workhorse for amide coupling (2–4, 10, 30–32). To complement this strategy, the decarboxylative Giese reaction utilizes the same feedstock for access to C(sp^3)-rich architecture. Thirteen coupling products (**48**–**60**) were successfully synthesized from 11 different amino acids with excellent yields, testifying to the modularity of the approach. As noted above, several substrates (**31**, **33**, **36**, **43**, **56**) provided superior yields with zinc nanopowder. A one-pot protocol that involves in situ RAE formation was also developed, taking advantage of a new activation reagent hexafluorophosphate *N*-hydroxyphthalimide tetramethyluronium (HITU, **11**) which was prepared on kilogram scale in collaboration with Asymchem (*SI Appendix*).

With a deeper understanding of the driving force and scope of this transformation, the reaction was finally transitioned to a DEL format as depicted in Fig. 4. The mechanistic data from Fig. 2 guided the selection of either a DNA-bound acrylate (with

excess acid) or a DNA-bound carboxylic acid (with excess acrylate) starting point. From a practical vantage point, we envisioned that capping the Michael acceptors on DNA could be advantageous in providing an additional tool for $C(sp^3)$–$C(sp^3)$ coupling. The zero-order dependence on both [RAE] and [acrylate] suggested that both scenarios were viable. Indeed, Fig. 4*A* shows that not only could the acrylate be employed as a limiting reagent, but its use obviated the need for adding Ni, a conclusion rationalized by our kinetic analysis of Fig. 2*C*. Since RAE is utilized in excess in such a scenario, RAE-based by-product formation would not affect the desired product yield (based on limiting acrylate) or the purity of a DNA-bound substrate. By analogy to solid-phase organic synthesis (63), DEL-based synthesis confers a similar advantage in being able to simply wash away by-products formed as a result of side reactions from excess components. Subsequent optimization of additives and solvents led to a 74% yield of adduct **62**. The optimal condition using limited Michael acceptor was demonstrated on several substrates (Fig. 4*A*, **31**, **46**, **60**) and obtained comparable yield (*vide supra*).

The realization of true DEL compatibility is depicted in Fig. 4*B* and commenced from an amine bound to a 14-base DNA headpiece (5′-5Phos/GAGTCA/iSp9/iUniAmM/iSp9/TGACTCCC-3′, commercial from LGC Biosearch Technologies) followed by acylation with an appropriate acid bearing an acrylate motif. Pleasingly, the conditions delineated above, after slightly tweaking the solvent and buffer (*SI Appendix*), translated well to a DEL-based setting, furnishing a diverse array of adducts (**63**–**84**). Notably, amino-containing, alkyl carboxylic acids (**63**, **64**, **68**–**72**, **74**, **75**, **78**, **82**–**84**), and even a dipeptide (**79**) could be employed. Highly hindered $C(sp^3)$–$C(sp^3)$ linkages (**65**–**67**, **73**, **76**, **77**, **80**, **81**) could also be constructed which represents a unique example of forging quaternary systems on DNA through cross-coupling. Thus, the DEL toolbox has now been expanded to include access to a broad variety of $C(sp^3)$-rich architectures.

Conclusion

In the original manifestation of DEL-based diversity synthesis, amide bond formation was the only known compatible reaction that could be employed. In the past two decades, great strides have been made to expand the toolbox of reaction modes that are compatible with the idiosyncratic aqueous, dilute, and DNA-sensitive parameters of this system. This work describes a systematic approach to translating standard organic reactions to a DEL setting through the tactical combination of kinetic analysis and empirical screening with information captured from data mining. To exemplify this model, a direct cross-coupling to forge high-value C–C bonds was studied, a transformation targeted to access scaffolds of intense interest in medicinal chemistry.

From a mechanistic standpoint, there are several general lessons gained from this study. First, when transitioning from organic to DEL-based synthesis, chemists should consider absolute concentrations rather than simply the number of equivalents in evaluating reaction driving forces. Secondly, temporal kinetic analysis can be a valuable modality for rapid assessment of factors leading to higher yield. Finally, a careful reactivity analysis of the coupling partners can lead to a judicious selection of the optimal DNA-bound substrate.

The DEL-based one-electron cross-coupling enabled herein is notable due to the current dogma that DNA is not compatible with the presence of pathways involving radical intermediates. Thus, in addition to diverse pathways incorporating pericyclic, carbonyl-based, and two-electron cross-coupling paradigms, radical-based reactions should also be considered in the planning stages and design of DELs.

Materials and Methods

All reagents and DNA headpiece were commercially available and used as supplied without further purification. The details of the materials, methods including synthesis and characterization of compounds, kinetic data analysis, reaction optimizations, and reactions on DNA are described in *SI Appendix*.

ACKNOWLEDGMENTS. We thank D.-H. Huang and L. Pasternack for assistance with NMR spectroscopy; Prof. B. Paegel for useful discussions and preliminary tests on DNA stability under DEL-like conditions; M. Hill and E. Costa for DNA analytic method development; Guanda Che, Denghui Bao, and En-Xuan Zhang (Asymchem) for large-scale preparation of HITU (**11**); and LGC Biosearch Technologies for preparing DNA headpiece. Financial support for this work was provided by Pfizer and NIH (Grant GM-118176). The Swedish Research Council, The Foundation Blanceflor Ludovisi née Bildt, Stiftelsen Olle Engkvist Byggmästare, and The Hans Werthén Fund Scholarship supported research fellowships (to H.L.), Uehara Memorial Foundation supported a research fellowship (to S.A.), and Agencia Canaria de Investigación, Innovación y Sociedad de la Información - Unión Europea supported a predoctoral fellowship (to P.M.-A.).

1. Brenner S, Lerner RA (1992) Encoded combinatorial chemistry. *Proc Natl Acad Sci USA* 89:5381–5383.
2. Nielsen J, Brenner S, Janda KD (1993) Synthetic methods for the implementation of encoded combinatorial chemistry. *J Am Chem Soc* 115:9812–9813.
3. Needels MC, et al. (1993) Generation and screening of an oligonucleotide-encoded synthetic peptide library. *Proc Natl Acad Sci USA* 90:10700–10704.
4. Kerr JM, Banville SC, Zuckermann RN (1993) Encoded combinatorial peptide library containing non-natural amino acid. *J Am Chem Soc* 115:2529–2531.
5. Gartner ZJ, et al. (2004) DNA-templated organic synthesis and selection of a library of macrocycles. *Science* 305:1601–1605.
6. Li G, Zheng W, Liu Y, Li X (2015) Novel encoding methods for DNA-templated chemical libraries. *Curr Opin Chem Biol* 26:25–33.
7. Neri D, Lerner RA (2018) DNA-encoded chemical libraries: A selection system based on endowing organic compounds with amplifiable information. *Annu Rev Biochem* 87: 5.1–5.24.
8. Mannocci L, et al. (2008) High-throughput sequencing allows the identification of binding molecules isolated from DNA-encoded chemical libraries. *Proc Natl Acad Sci USA* 105:17670–17675.
9. Scheuermann J, Neri D (2015) Dual-pharmacophore DNA-encoded chemical libraries. *Curr Opin Chem Biol* 26:99–103.
10. Franzini RM, Randolph C (2016) Chemical space of DNA-encoded libraries. *J Med Chem* 59:6629–6644.
11. Franzini RM, Neri D, Scheuermann J (2014) DNA-encoded chemical libraries: Advancing beyond conventional small-molecule libraries. *Acc Chem Res* 47:1247–1255.
12. Lerner RA, Brenner S (2017) DNA-encoded compound libraries as open source: A powerful pathway to new drugs. *Angew Chem Int Ed* 56:1164–1165.
13. Kleiner RE, Dumelin CE, Liu DR (2011) Small-molecule discovery from DNA-encoded chemical libraries. *Chem Soc Rev* 40:5707–5717.
14. Buller F, Mannocci L, Scheuermann J, Neri D (2010) Drug discovery with DNA-encoded chemical libraries. *Bioconjug Chem* 21:1571–1580.
15. Satz AL (2018) What do you get from DNA-encoded libraries? *ACS Med Chem Lett* 9: 408–410.
16. Goodnow RA, Jr (2014) *A Handbook for DNA-Encoded Chemistry: Theory and Applications for Exploring Chemical Space and Drug Discovery,* (Wiley, New York).
17. Ding Y, et al. (2015) Discovery of potent and selective inhibitors for ADAMTS-4 through DNA-encoded library technology (ELT). *ACS Med Chem Lett* 6:888–893.
18. Deng H, et al. (2013) Discovery of clinical candidate GSK1842799 as a selective S1P1 receptor agonist (prodrug) for multiple sclerosis. *ACS Med Chem Lett* 4:942–947.
19. Kollmann CS, et al. (2014) Application of encoded library technology (ELT) to a protein-protein interaction target: Discovery of a potent class of integrin lymphocyte function-associated antigen 1 (LFA-1) antagonists. *Bioorg Med Chem* 22:2353–2365.
20. Machutta CA, et al. (2017) Prioritizing multiple therapeutic targets in parallel using automated DNA-encoded library screening. *Nat Commun* 8:16081–16090.
21. Gartner ZJ, Liu DR (2001) The generality of DNA-templated synthesis as a basis for evolving non-natural small molecules. *J Am Chem Soc* 123:6961–6963.
22. Li X, Liu DR (2004) DNA-templated organic synthesis: nature's strategy for controlling chemical reactivity applied to synthetic molecules. *Angew Chem Int Ed* 43:4848–4870.
23. Breaker RR, Joyce GF (2014) The expanding view of RNA and DNA function. *Chem Biol* 21:1059–1065.
24. Burrows CJ, Muller JG (1998) Oxidative nucleobase modifications leading to strand scission. *Chem Rev* 98:1109–1152.
25. Malone ML, Paegel BM (2016) What is a "DNA-compatible" reaction? *ACS Comb Sci* 18:182–187.
26. Clark MA, et al. (2009) Design, synthesis and selection of DNA-encoded small-molecule libraries. *Nat Chem Biol* 5:647–654.
27. Satz AL, et al. (2015) DNA compatible multistep synthesis and applications to DNA encoded libraries. *Bioconjug Chem* 26:1623–1632.
28. Averick SE, Dey SK, Grahacharya D, Matyjaszewski K, Das SR (2014) Solid-phase incorporation of an ATRP initiator for polymer-DNA biohydrides. *Angew Chem Int Ed* 53:2739–2744.

29. Goodnow RA, Jr, Dumelin CE, Keefe AD (2017) DNA-encoded chemistry: Enabling the deeper sampling of chemical space. *Nat Rev Drug Discov* 16:131–147.
30. Seigal BA, et al. (2015) The discovery of macrocyclic XIAP antagonists from a DNA-programmed chemistry library, and their optimization to give lead compounds with in vivo antitumor activity. *J Med Chem* 58:2855–2861.
31. Heinis C, Winter G (2015) Encoded libraries of chemically modified peptides. *Curr Opin Chem Biol* 26:89–98.
32. Li Y, et al. (2018) Versatile protein recognition by the encoded display of multiple chemical elements on a constant macrocyclic scaffold. *Nat Chem* 10:441–448.
33. Ding Y, Clark MA (2015) Robust Suzuki-Miyaura cross-coupling on DNA-linked substrates. *ACS Comb Sci* 17:1–4.
34. Lu X, Fan L, Phelps CB, Davie CP, Donahue CP (2017) Ruthenium promoted on-DNA ring-closing metathesis and cross metathesis. *Bioconjug Chem* 28:1625–1629.
35. Gartner ZJ, Kanan MW, Liu DR (2002) Expanding the reaction scope of DNA-templated synthesis. *Angew Chem Int Ed* 41:1796–1800.
36. Buller F, et al. (2009) Discovery of TNF inhibitors from a DNA-encoded chemical library based on Diels-Alder cycloaddition. *Chem Biol* 16:1075–1086.
37. Reactions CA (1992) *Organic Synthesis*, ed Perlmutter P (Pergamon, Oxford).
38. Rossiter BE, Swingle NM (1992) Asymmetric conjugate addition. *Chem Rev* 92: 771–806.
39. Gerry CJ, Schreiber SL (2018) Chemical probes and drug leads from advances in synthetic planning and methodology. *Nat Rev Drug Discov* 17:333–352.
40. Shi B, Zhou Y, Huang Y, Zhang J, Li X (2017) Recent advances on the encoding and selection methods of DNA-encoded chemical library. *Bioorg Med Chem Lett* 27: 361–369.
41. Krasovskiy A, Duplais C, Lipshutz BH (2009) Zn-mediated, Pd-catalyzed cross-couplings in water at room temperature without prior formation of organozinc reagents. *J Am Chem Soc* 131:15592–15593.
42. Vidal C, García-Álvarez J, Hernán-Gómez A, Kennedy AR, Hevia E (2014) Introducing deep eutectic solvents to polar organometallic chemistry: Chemoselective addition of organolithium and Grignard reagents to ketones in air. *Angew Chem Int Ed* 53: 5969–5973.
43. Petrier C, Dupuy C, Luche JL (1986) Conjugate additions to α,β-unsaturated carbonyl compounds in aqueous media. *Tetrahedron Lett* 27:3149–3152.
44. Luche JL, Allavena C (1988) Ultrasound in organic synthesis 16. Optimisation of the conjugate additions to α,β-unsaturated carbonyl compounds in aqueous media. *Tetrahedron Lett* 29:5369–5372.
45. Wright TH, et al. (2016) Posttranslational mutagenesis: A chemical strategy for exploring protein side-chain diversity. *Science* 354:aag1465.
46. Yang A, et al. (2016) A chemical biology route to site-specific authentic protein modifications. *Science* 354:623–626.
47. Qin T, et al. (2016) A general alkyl-alkyl cross-coupling enabled by redox-active esters and alkylzinc reagents. *Science* 352:801–805.
48. Li C, et al. (2017) Decarboxylative borylation. *Science* 356:eaam7355.
49. Edwards JT, et al. (2017) Decarboxylative alkenylation. *Nature* 545:213–218.
50. Qin T, et al. (2017) Nickel-catalyzed Barton decarboxylation and Giese reactions: A practical take on classic transforms. *Angew Chem Int Ed* 56:260–265.
51. Bloom S, et al. (2018) Decarboxylative alkylation for site-selective bioconjugation of native proteins via oxidation potentials. *Nat Chem* 10:205–211.
52. McCarver SJ, et al. (2017) Decarboxylative peptide macrocyclization through photoredox catalysis. *Angew Chem Int Ed* 56:728–732.
53. Blackmond DG (2005) Reaction progress kinetic analysis: A powerful methodology for mechanistic studies of complex catalytic reactions. *Angew Chem Int Ed* 44:4302–4320.
54. Mathew JS, et al. (2006) Investigations of Pd-catalyzed ArX coupling reactions informed by reaction progress kinetic analysis. *J Org Chem* 71:4711–4722.
55. Blackmond DG (2015) Kinetic profiling of catalytic organic reactions as a mechanistic tool. *J Am Chem Soc* 137:10852–10866.
56. Okada K, Okamoto K, Oda M (1988) A new and practical method of decarboxylation: Photosensitized decarboxylation of N-acyloxyphthalimides via electron-transfer mechanism. *J Am Chem Soc* 110:8736–8738.
57. Cornella J, et al. (2016) Practical Ni-catalyzed aryl-alkyl cross-coupling of secondary redox-active esters. *J Am Chem Soc* 138:2174–2177.
58. Lee S, Lim CJ, Kim S (2004) Decarboxylative allylation and vinylation approach of thiohydroxamate esters. *Bull Korean Chem Soc* 25:1611–1612.
59. Chalmers BA, et al. (2016) Validating Eaton's hypothesis: Cubane as a benzene bioisostere. *Angew Chem Int Ed* 55:3580–3585.
60. Gianatassio R, et al. (2016) Strain-release amination. *Science* 351:241–246.
61. Stepan AF, et al. (2012) Application of the bicyclo[1.1.1]pentane motif as a nonclassical phenyl ring bioisostere in the design of a potent and orally active γ-secretase inhibitor. *J Med Chem* 55:3414–3424.
62. Myers MR, et al. (2003) Potent quinoxaline-based inhibitors of PDGF receptor tyrosine kinase activity. Part 1: SAR exploration and effective bioisosteric replacement of a phenyl substituent. *Bioorg Med Chem Lett* 13:3091–3095.
63. Solid-Phase Organic Synthesis (2011) *Concepts, Strategies, and Applications*, eds Toy RH, Lam Y (Wiley, New York).